Fluorescence, thermal and mechanical properties of PMMA-CdSe QD film

H. EL-SWIE[a], I. RADOVIC[a], D. B. STOJANOVIC[a], D. M. SEVIC[b], M. S. RABASOVIC[b], P. USKOKOVIC[a], V. RADOJEVIC[a*]
[a]*University of Belgrade, Faculty of Technology and Metallurgy, Belgrade*
[b]*University of Belgrade, Institute of Physics, Zemun, Serbia*

In the present paper an effort has been made to investigate processing and characterization of composite poly (methyl methacrylate)-cadmium selenide (PMMA-CdSe). Thin films of pure PMMA and composites with 0.06 % wt. CdSe quantum dots nanoparticles were made using solution casting method. Characterization of starting components and composites was performed in order to obtain information of their morphology, structure, thermal stability, mechanical and optical properties. Nanoindentation revealed mechanical improvements with the addition of the crystal through reduced elastic modulus and hardness values. DSC analysis has shown an increase in T_g for composite with CdSe. Optical studies by time resolved laser induced fluorescence (TR-LIF) showed that the size-tunable optical properties can be achieved in the polymer films by addition of quantum dots.

(Received October 28, 2016; accepted April 6, 2017)

Keywords: Electrospinning, Composite polymer nanofibers, Quantum dots, Fluorescence

List of abbreviations

PMMA	poly (methyl methacrylate)
CdSe	Cadmium Selenide
DMF	Dimethylformamide
QD	Quantum dots
Mw	Molecular Weight
n	index of refraction
λ	wave lenght
DSC	Differential Scanning Calorimetry
FTIR	Fourier transform infrared spectroscopy
FESEM	Field Effective Scanning Electron Microscope
TR LIF	time resolved laser induced fluorescence
OPO	Optical Parametric Oscillator laser

1. Introduction

Nanocomposite polimer films doped with QD have many commercial or potential applications in biological labeling and diagnostics, LED's, electro-luminescent devices, photovoltaic devices, lasers and single electrode transistors [1–5]. High performance in polymer blends and composites can be achieved by addition of a nano size filler component into a polymer matrix. In this regard polymer nanocomposites present a promising alternative of conventional composites. Recently, studies on blends of immiscible polymers containing nanoparticles have attracted the attention of several research groups [6-9]. These studies suggest that under certain conditions the polymer molecules and the nanoparticles should not be regarded as individual entities within the blend, but instead as complex aggregates.

Polymeric nanocomposites consisting of inorganic nanoparticles and organic polymers represent a new class of materials that exhibit different performance compared to their microparticle counterparts. The properties of polymer composites depend on the type of nanoparticles that are incorporated, their size and shape.

Poly (methyl methacrylate) (PMMA), a transparent thermoplastic polymer, has been widely used in many commercial applications due to his high impact-resistance, ease of fabrication, low density, and cost-effective technologies. [10]. For example, PMMA has been one of the most popular substrate materials in making polymer-based micro fluidic devices to perform chemical and biological assays due to its excellent chemical, physical, biological, mechanical, optical and thermal properties [11-13].

Semiconductor nanoparticles are notable for their wide fundamental research and industrial applications [14, 15]. Their defining characteristic is their size which is in the range of 1–100nm and excellent chemical processibility. The strong confinement of excited electrons and holes leads to dramatically different optical and electronic properties compared to the bulk semiconductor [16]. Many studies have been made on III–V and II–VI semiconductor quantum dots (QDs) all over the world. For II–VI QDs, CdSe QDs prepared by chemical methods are the most popular [17]. Many studies have been focused on CdSe QDs because of its high luminescence quantum yield, narrow band gap and a variety of optoelectronic conversion properties compared to bulk CdSe [18].

Polymer nanocomposites with QDs have a wide range of applications in optoelectronics and biosensing as solar cells, light emitting diodes and bio-labeling [19, 20]. Those nanocomposites are usually used in film form in which the distance between QDs in polymer matrix is fixed. Inter-particle distance between QDs in film plays a crucial role in determining the quantum yield of fluorescence. QDs in polymer matrix usually aggregates in clusters and reduced quantum yield, so it is important to control both dispersion and film production process to retain its initial quantum yield [21–25]

In this paper the thermal and mechanical properties of nanocomposite film PMMA-CdSe beside fluorescence are investigated. Those results could help in design of processing and efficiency of advanced optical nanocomposite films and provide the possibility to maintain combinations of functionalities, such as thermally conducting composites with good mechanical properties that are optically clear.

2. Experimental details

2.1. Materials

Commercially available PMMA Acryrex® CM205 (Chi Mei Corp. Korea, (Mw≈90400 g/mol, n = 1.49, λ = 633 nm) pellets were used as a matrix for preparing samples. The quantum dots of cadmium selenide (CdSe) nanoparticles, were supplied from QD particles, Future Chemistry, Netherland, 610nm, a solution in toluene. Dimethylformamide (DMF, anhydrous, 99.8%, Sigma-Aldrich) was used as solvent.

2.1.1. Preparation of PMMA and CdSe-PMMA Films

In the preparation of precursor solutions, DMF was used as the solvent for the PMMA. In a typical process, homogenous solution of polymer with respect to the amount of composite films was prepared by dissolving the polymeric granules (PMMA, m=10.65g) in 40 ml of DMF under magnet stirring for 48 h at room temperature on the mixture. The concentration of PMMA in DMF solution was 22 % wt. PMMA was therefore produced in form of film by solvent casting method, i.e. casting the resulting PMMA solution which we previously prepared on Petri dish in horizontal position. The solution was air dried for 24 h at room temperature and the obtained film was kept for further 24h in dryer under 60 ºC in order to eliminate residual solvent.

For the synthesis of polymer/quantum dots (PMMA/ CdSe) composite films the procedure for solutions was similar. The concentration of PMMA in DMF solution was 22 % wt. The concentration of CdSe particles in films was 0.06 % wt. which prepared by dispersed CdSe particles in toluene, being the powder. The resulting suspension was directly added to PMMA solution previously prepared. The mixture was stirred for 24 h. The same procedure we did with CdSe-PMMA solution, i.e. casting CdSe-PMMA solution on Petri dish by placed it on Petri dish, and then the spacemen was dried for 24 h at room temperature and further drier for 24 h in dryer oven under 60 ºC.

2.1.2. Characterization of samples

Infrared (IR) spectrum of the pure PMMA and the composites were obtained with a Fourier transform infrared (FTIR) transmission-KBr disk spectroscopy, Hartmann & Braun, MB-series. The scanning range of FTIR was between 4000 and 400 cm^{-1} with a resolution of 4 cm^{-1}.

Differential scanning calorimetry (DSC) TA instruments Q10 analysis was done under the nitrogen purge at a flow rate of 50 mL/min. Each sample was first heated from room temperature to 150 °C with a heating rate of 10 °C/min to remove thermal history, followed by cooling down to 40 °C and then reheating to 150 °C at the same cooling rate to determine the glass transition temperature. The sample weight was about 5-6 mg. DSC scans were analyzed by TA Instruments Universal Analysis Software. The class transition temperature is recorded according to the most commonly accepted way in literature, i.e., the midpoint of the heat flow (capacity) step transition between the glass and rubbery states.

An insight of dispersion and deagglomeration of nanoparticles was performed using FESEM (TESCAN MIRA 3) with fracture surfaces sputtered with gold.

The nanoindentation test was performed using a Hysitron TI 950 TriboIndenter equipped with in situ SPM imaging (Hysitron, MN). The geometry of a Berkovich tip can be described as a three-sided pyramidal tip with a total included angle of 142.35 º and a half-angle of 65.35 º. The Berkovich indenter has an average radius of curvature of about 100 nm. Indentation testing at nanoscale was used to investigate the nanomechanical properties, including indentation hardness (H), reduced elastic modulus (E_r), of the neat PMMA and nanocomposites. The tests were performed in the force controlled feedback mode. The indentation maximum load was set at 2 mN for each tested sample. The loading and unloading times as well as the hold time at the peak force were set to 25 s each. For each loading /hold /unloading cycle, the applied load value was plotted with respect to the corresponding position of the indenter. The resulting load/displacement curves provide data specific to the mechanical nature of the material under examination. All the results were obtained by the Oliver and Pharr method [26].

The time-resolved laser induced fluorescence measurement system used in this work consists of Nd-YAG Vibrant OPO (Optical Parametric Oscillator) laser and Hamamatsu streak camera, described in [27], as shown in Fig. 1. The output of the OPO can be continuously tuned from 320 nm to 475 nm, enabling us to determine the optimal excitation wavelength of measured samples. After analysis of the preliminary results, the OPO output tuned at 330 nm was used as the excitation source of the samples. For measurements presented here the output energy of OPO was about 5 mJ. Time-resolved streak images of the fluorescence spectra, obtained by

spectrograph (SpectraPro-2300i), were taken by streak camera in photon counting mode. The spectrograph grating of 50 lines/mm was used covering a wide spectral range of 330 nm. The streak images were acquired and analyzed using the HPD-TA (High Performance Digital Temporal Analyzer) streak camera control software. Fluorescence lifetime fitting analysis was carried out using the TA-Fit program.

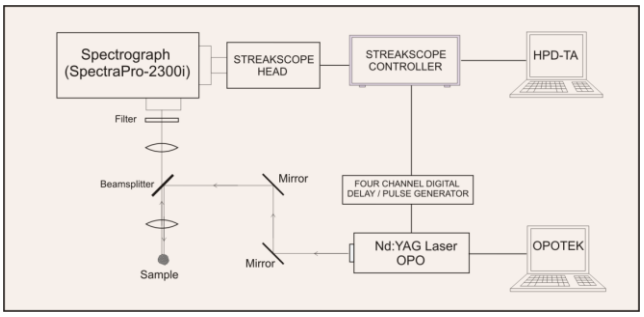

Fig 1. The time-resolved laser induced fluorescence measurement system, where the excitation and detection optical axes are collinear

Our preliminary analysis of QD samples in liquid solution and PMMA films was performed in usual geometry, with the detector set 90 degrees to the light source, but the better quality of measurements (regarding the intensity of optical response, usefulness of comparison of liquid sample and PMMA film) was achieved when the fluorescence emission was collected in the reflective mode with the small angle between excitation and detection axes. So, finally, the fluorescence emission was collected at axis collinear to the excitation axis, using beam splitter, as shown in Fig. 1. The filter in front of spectrograph blocks the light around the excitation wavelength. It could be seen in Fig. 1. that it is easy to tune the angle of excitation beam by moving the mirrors which guide the laser beam.

3. Results and discussion

The PMMA film and nanocomposite have been further characterized with FTIR (Fig.2) to determine if any changes in functionality occurred in the composite film due to chemical interactions between the PMMA and the quantum dots. Spectrum of PMMA exhibits typical vibrational bands, *i.e.*, vibrational bands at 986 and 1453 cm^{-1} that belong to O–CH_3 bending and the stretching deformation of PMMA, respectively, bands at 1732 and 1250 cm^{-1} that are assigned to the stretching of C=O groups, a band at 1065 cm^{-1} that could be ascribed to the C–O stretching vibration and a band at 1197 cm^{-1} that belongs to the skeletal chain vibration. The other bands appearing in 3000 – 2800 cm^{-1}, 1490 – 1275 cm^{-1} and 900 – 750 cm^{-1} spectral regions correspond to different CH_3 and CH_2 vibrational modes [28, 29].

The spectra of pure PMMA and of CdSe/PMMA nanocomposite are almost identical. All of the stretching vibrations observed in the PMMA appeared in the nanocomposite with a higher intensity. A band at 624 cm^{-1} is due to the stretching frequency of Cd–Se bond [30].

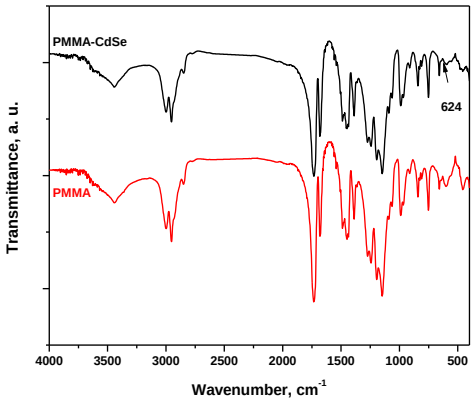

Fig. 2. FTIR spectrum of pure PMMA film and PMMA/CdSe film

FESEM photos of the fracture surfaces of composite films with QD particles are presented in Fig. 3. As could be seen, some level of the agglomeration of QD is presented.

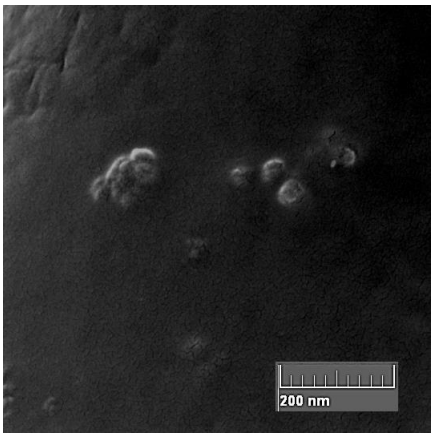

Fig. 3. FESEM of composite film surface

Results of DSC for pure PMMA and composite are presented in Fig. 4. The phase behavior of the polymer nanocomposite affected by an inclusion of a small fraction of QDs was exploited in a DSC by checking the glass transition temperature T_g change. Thermal analysis presented on Fig. 4 shows that there is around 1% increase in Tg value for PMMA-CdSe nanocomposite, compared to the pure PMMA film. This finding has revealed that the agglomerates of QDs did not disrupt mechanical properties of the polymer. A small increase in T_g suggested that QDs behave as a functional physical crosslink, which would confirm the absence of a covalent bond between the polymer and the particles assumed by the FTIR analysis.

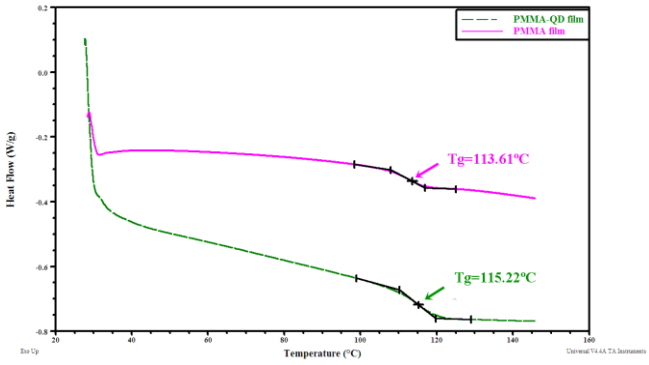

Fig. 4. DSC of pure PMMA and the composite

In order to obtain an overview of the possible inhomogenity in the sample, nanoindentation measurements were performed on nine positions for every sample. Fig. 5 shows typical force–depth curves obtained in the nanoindentation tests for neat PMMA film and a composite with CdSe. The curves appear to be with continuity and without pop-in or pop-out in both loading and unloading phases. Fig. 5 b) displays the plastic imprint of the indent for the sample with QD particles. In-situ imaging mode used for scanning the surface trace reveals the absence of cracks and fractures around the indent. The relative increase of reduced elastic modulus and hardness compared to the neat PMMA was 3.8 % and 15.9 % respectively (Table 1). The hardness (*H*) of a material is a measure of its resistance to shear stresses under local volume compression. The increased resistance to surface deformation of the PMMA nanocomposite may be due to a decrease in the free volume of the matrix associated with the formation of apparent physical crosslinking and the entanglements. This increase of the hardness is in the agreement with the increase of T_g because both of them are closely related to the cohesive energy density of the polymer [31-33].

Table 1. Results of nanoindentation test

Sample	Er, GPa	StDev, GPa	H, GPa	St Dev, GPa
PMMA	5.528861	0.320653	0.327145	0.022659
PMMA-CdSe	5.742875	0.282497	0.379106	0.023848

Streak images of fluorescence spectra of CdSe QDs liquid solution (as received) and CdSe QD/PMMA film are shown in Fig. 6. The images, recorded as a 2D matrix, enable both lifetime and fluorescence spectral characteristics analysis of the samples.

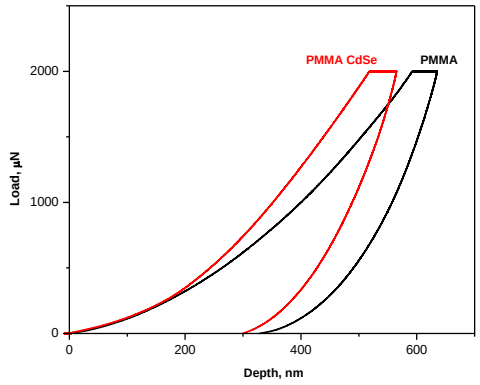

a)

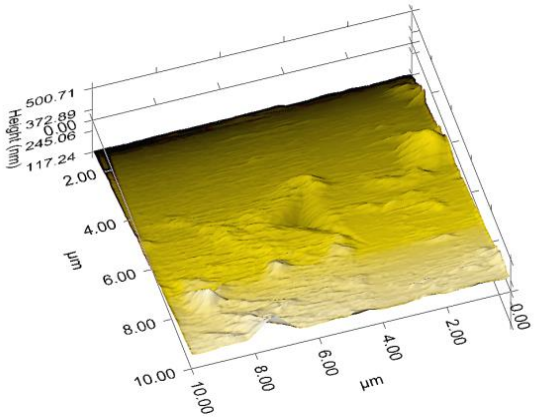

b)

Fig. 5. a) Force–depth curves obtained by nanoindentation, for pure PMMA and composite films, b) The plastic imprint of the indent for the sample with QD particles

Fluorescence emission peak of CdSe QDs liquid solution (Fig. 6a) is at 610 nm, as expected, because quantum dots with such fluorescence characteristics were obtained and used in this study. The typical nanosized CdSe is a cluster of several smaller nanocrystals. Due to extremely small dimension and high surface energy, these nanocrystallites agglomerate to give a resultant average size [34,35]. For CdSe QD/PMMA film (Fig 6b), there is a slight blue shift (peak is at 606 nm) due to a deagglomeration of some of the quantum dots during the process of the fabrication of the film.

The fluorescence lifetime of CdSe QD liquid solution and CdSe QD/PMMA film was calculated, obtaining the values of 1.8 ns and 2.1 ns respectively. The fluorescence lifetime of analyzed CdSe QD material is slightly increased when quantum dots are hosted in PMMA.

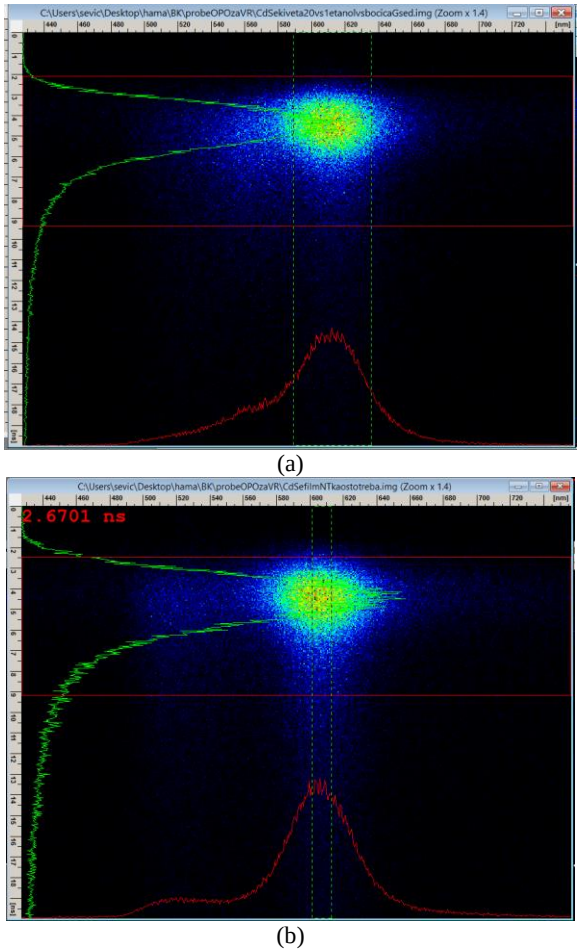

(a)

(b)

Fig. 6. Streak images of fluorescence spectra of a) CdSe QD liquid solution and b) CdSe QD/PMMA film

4. Conclusion

This study reports the preparation of composites with PMMA doped with CdSe QDs mechanical properties utilizing the solution casting technique. The results obtained from the DSC showed that on the addition of QDs, T_g value of the PMMA slightly increased, suggesting that the nanoparticles formed aggregates which have not disrupted mechanical performance of the polymer. The time resolved analysis of the nanocomposites revealed that the fluorescence of the powder was preserved in the composite. The fluorescence lifetime of PMMA doped with QDs has also slightly increased. As shown by the nanoindentation tests, incorporation of 3 wt % of QDs increased the reduced modulus and the hardness of PMMA composite for 3.8 % and 15.9 %, respectively. Studies of CdSe QDs in polymer matrices are in progress and lead to understanding more about the phenomenology in optical behavior in interface between the CdSe QDs and the host matrices for purposes of future applications of QDs-polymer composites in optoelectronic and photonic devices. The presented results suggested that PMMA/QD nanocomposites have good potential for the use in light sensitivity elements and optoelectronic devices, because the optical activity of QD is prevented in polymer medium, while the mechanical and thermal properties were improved.

Acknowledgement

This work was supported by the Ministry of Education, Science and Technology Development of the Republic of Serbia, Project Nos. TR 34011, III 45019 and 171020

Refrences

[1] S. Coe, W. K. Woo, M. Bawendi, Bulovic V. Nature **420**, 800 (2002).
[2] A. A. Mamedov, A. Belov, M. Giersig, N. N. Mamedova, N. A. Kotov, J. Am. Chem. Soc. **123,** 7738 (2001).
[3] M. Bruchez, M. Moronne, P. Gin, S. Weiss, A. P. Alivisatos, Science **281**, 2013 (1998).
[4] N. Charve, P. Reiss, A. Roget, A. Dupuis, D. Grundwald, S. Crayon, F. Chandezon, T. Livache, J. Mater. Chem. **14**, 2638 (2004).
[5] Y. Xuan, D. Pan, N. Zhao, X. Ji, D. Ma, Nanotechnology **17**, 4966 (2006)
[6] V. V. Ginzburg, F. Qiu, M. Paniconi, G. Peng, D. Jasnow, A. C. Balazs, Phys. Rev. Lett. **82**, 4026 (1999). doi:10.1103/PhysRevLett.82.4026
[7] Y. Tang, T. J. Ma, Chem. Phys. **116**, 7719 (2002).
[8] M. Laradji, G. J. MacNevin, Chem. Phys. **119**, 2275 (2003).
[9] C. Minelli, I. Geissbuehler, R, Eckert, H. Vogel, H. Heinzelmann, M. Liley, Colloid Polym. Sci. **282**, 1274 (2004). doi:10.1007/s00396-004-1070-y
[10] H. R. Allcock, J. D. Bender, Y. Chang, Chem. Mater. **15**, 473 (2003).
[11] C. Lu, B. Yang, J. Mater. Chem. **19**, 2884 (2009).
[12] S. A. Soper, S. M. Ford, S. Qi, R. L. McCarley, K. Kelly, M. C. Murphy, Anal. Chem. **72**, 642 (2000).
[13] R. L. McCarley, B. Vaidya, S. Wei, A. F. Smith, A. B. Patel, J. Feng, M. C. Murphy, S. A. Soper, J. Am. Chem. Soc. **127**, 842 (2005).
[14] Y. Dongzhi, C. Qifan, X. Shukun, J. Lumin. **126**, 853 (2007).
[15] X. G. Peng, J. Wickham, A. P. Alivisatos, J. Am. Chem. Soc. **120**, 5343 (1998).
[16] M. Green, P. O'Brien, Chem. Commun. **22**, 2235 (1999).
[17] Y. Xie, W. Z. Wang, Y. T. Qian, X. M. Liu, J. Solid State Chem. **147**, 82 (1999).
[18] J. J. Zhu, O. Palchik, S. Chen, A. Gedanken, J. Phys. Chem. B **104**, 7344 (2000).
[19] L. Liu, Q. Peng, Y. Li, Inorg. Chem. **47**, 5022 (2008).
[20] C. B. Murray, C. R. Kagan, M. G. Bawendi, Science **270**, 1335 (1995).
[21] K. Tai, W. Lu, I. Umezu, A. Sugimura, Appl. Phys. Express **3**, 035202 (2010).

[22] H. C. Kim, H. G. Hong, C. Yoon, H. Choi, I. S. Ahn, D. C. Lee, Y. J. Kim, K. Lee, J. Colloid Interf. Sci. **393**, 74 (2013).
[23] D. Qi, M. Fischbein, M. Drndic, S. Selmic, Appl. Phys. Lett. **86**, 093103 (2005).
[24] O. O. Akinwunmi, G. O. Egharevba, E. O. B. Ajayi, J. Mod. Phys. **5**, 257 (2014).
[25] I Suarez, H Gordillo, R Abargues, S Albert, J. Mart, I. Pastor, Nanotechnology **22**, 435202 (8pp) (2011). doi:10.1088/0957-4484/22/43/435202
[26] W. C. Oliver, G. M. Pharr, J. Mater. Res. **7**, 1564 (1992).
[27] M. S. Rabasovic, D. Sevic, M. Terzic, B. P. Marinkovic, Nucl. Instrum. Meth. B. **279,** 16 (2012).
[28] I. S. Elashmawi, N. A. Hakeem, Polym. Eng. Sci. **48**, 895 (2008).
[29] G. Socrates, Infrared and Raman Characteristic Group Frequencies, New York: Wiley (2001).
[30] A. Acharya, R. Mishra, G. S. Roy, Lat. Am. J. Phys. **4**, 603 (2010).
[31] F. J. Baltá-Calleja, A. Flores, F. Ania, in Mechanical properties of polymers based on nanostructure and morphology, G. H. Michler, F. J. Baltá-Calleja, Eds., London:Taylor and Francis (2005).
[32] A.Flores, F. Ania, F. J. Baltá-Calleja, Polymer **50**, 729 (2009).
[33] S. S.Musbah, V. Radojević**,** N. Borna, D. Stojanović, M. Dramićanin, A. Marinković, R. Aleksić, J. Serb. Chem. Soc. **76**, 1153 (2011).
[34] N. A. Hamizi, M. R. Johan, Mater. Chem. Phys. **124**, 395 (2010).
[35] J. Yao, G. Zhao, D. Wang, G. Han, Mater. Lett. **59**, 3652 (2005).

*Corresponding author: vesnar@tmf.bg.ac.rs